

Backscatter ratios using lidar sounding over Tomsk and Hefei

Zhenzhu Wang^{*,a}, Anatoli G. Borovoi^b, Dong Liu^a, Chenbo Xie^a, Yuri S. Balin^b, Grigorii P. Kokhanenko^b, Alexander V. Konoshonkin^b, Natalia V. Kustova^b, Sergey V. Nasonov^b

^aKey Laboratory of Atmospheric Composition and Optical Radiation, Anhui Institute of Optics and Fine Mechanics, Chinese Academy of Sciences, Hefei 230031, P. R. China

^bV. E. Zuev Institute of Atmospheric Optics, Rus. Acad. Sci, Tomsk, 634055, Russia

*zzwang@aiofm.ac.cn; phone 13855171045

ABSTRACT

Cirrus clouds cover about 30% of the Earth surface and they essentially impact on the radiative budget of the Earth and, consequently, on the climate. This study investigated the properties of cirrus cloud by used observations obtained from the three-wavelength lidar system over Tomsk and Hefei. The backscatter ratios (polarization ratio, color ratio and lidar ratio) for cirrus cloud are compared with each other from these two regions. Some differences are found that are caused by aerosol conditions. These differences have been mitigated by use of the appropriate microphysical model.

Keywords: Lidar, cirrus cloud, Tomsk, Hefei

1. INTRODUCTION

Cirrus clouds play essential role in the radiative balance of the system Earth-atmosphere. At present, they are one of the main sources of uncertainties appearing in the up-to-date numerical models of the Earth's circulation and global climate change. Indeed, though cirrus clouds are often optically thin, they cover in average 30% of the Earth surface, the coverage being 60% – 70% in tropics [1-3]. They consist mainly of ice crystals and are localized at high altitudes where the temperature is low. Therefore they effectively trap the thermal infrared radiation causing the warming effect like the warming effect of the green-house gases. On the other hand, if the clouds become optically thick, they reflect the solar radiation causing the cooling effect. It was proved that the warming/cooling influence of cirrus clouds on the Earth climate depends, besides their optical depth, on sizes and shapes of the ice crystals, too. These microphysical characteristics of cirrus clouds (sizes, shapes, spatial orientation, number density and their vertical profiles) are poorly studied until now because of their strong spatial and temporal variability. The backscatter ratios (polarization ratio, color ratio and lidar ratio) for cirrus have been focused on in experiment [4-9] and theory [10-13]. But these properties for cirrus clouds detected from different regions along the world are not investigated in detail. Fortunately, the multi-wavelength Polarization Lidars have been set for cirrus cloud backscatter ratios measurement over Hefei and TOMSK. In this paper, we present the lidar system and the retrieved method in section 2 and some compared results will be described in section 3. Section 4 gives the conclusions and discussions.

2. LIDAR SYSTEMS AND METHODS

We have performed simultaneous measurements of the attenuated color ratio, the polarization parameter and lidar ratio in cirrus clouds in Tomsk, Russia, by use of the two-wavelength polarization lidar LOSA-S described earlier [14]. An LS-2137 laser (Nd: YAG, 532 nm) with energy per pulse of 300 mJ and pulse repetition frequency of 10 Hz was used in this lidar system. The receiver antenna is the Cassegrainian telescopic system ($D = 0.2$ m and $f = 2$ m). The field stop forms a field-of-view (FOV) angle of 1 mrad. The Wollaston prism (WP), forming two beams with mutually orthogonal polarization states, is inserted into the scattered beam path. Two FEU-84 PMTs and one APD were used as receivers. At the meanwhile, the TRMPL [15] is a moveable and continuous working lidar installed in a standard container with a glass window on the roof. A three-wavelength Nd: YAG laser (Quantel Brilliant B) was equipped as the transmitter with a repetition of 10 Hz, and the laser energy is 160 mJ, 260 mJ and 280 mJ at the wavelength of 355 nm, 532 nm and 1064 nm, respectively. Three Mie scattering (355 nm, 532 nm and 1064 nm) and one depolarization (532 nm) signals were collected by the telescope (Meade Cassegrain LX400-ACF-14", $D = 0.35$ m and $f = 3.5$ m) simultaneously with the FOV of 0.5 mrad. The Licel PMT-detector modules are used for detecting 355 nm and 532 nm wavelengths (including

parallel and perpendicular polarization components) and an APD-detector module is used for 1064 nm. A glass with a self-designed heater was covered on the roof window to get rid of the dew especially before the sunrise to ensure it could work under all weather conditions. The Range-corrected signals of the 1064 nm channels from TOMSK and Hefei were shown in Fig.1 and Fig. 2.

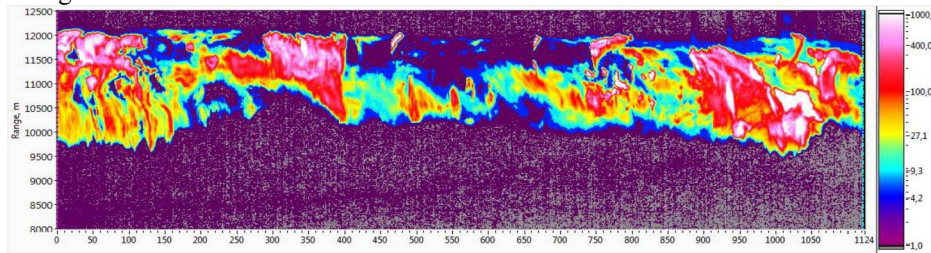


Figure 1. Range-corrected signal for 1064 receiving channel by LOSA-S.

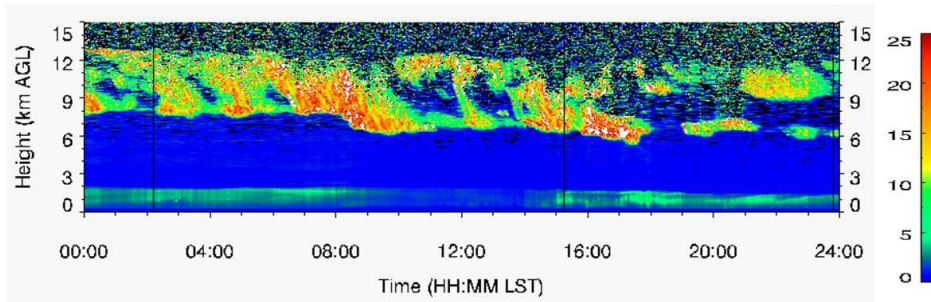


Figure 2. Range-corrected signal for 1064 receiving channels by TRMPL.

From Fig. 1 and Fig. 2, one can see two lidars worked continuously for cirrus clouds detecting. Structure of a layer of crystal clouds recorded in details with each polarization lidar. The scales in artificial colors for the corresponding signals are shown to the right of the figure. These signals are used for backscatter ratios.

The basic quantities characterizing the cirrus microphysics are the backscatter cross section σ_π and the extinction cross-section σ_e of the crystals that can be retrieved, in principle, from experimental data. Instead of these quantities, the following three dimensionless ratios are often used for interpreting the lidar experimental data:

$$\chi = \frac{\sigma_{\pi,\lambda1}}{\sigma_{\pi,\lambda2}} = \frac{\beta_{c,\lambda1}}{\beta_{c,\lambda2}} \approx \frac{\beta'_{c,\lambda1}}{\beta'_{c,\lambda2}} \quad (1)$$

Here, χ is the color ratio for the two wavelengths $\lambda1$ and $\lambda2$, β_c is cirrus cloud backscatter coefficient for the two wavelengths $\lambda1$ and $\lambda2$. For optically thick cirrus clouds [8], the cirrus cloud backscatter color ratios can be approximately reduced to the ratio of attenuated backscatter coefficient, which is usually true. But it ignores the attenuation that caused by aerosols.

$$L = \frac{\sigma_e}{\sigma_\pi} = \frac{\alpha_c}{\beta_c} \quad (2)$$

Here, L is the lidar ratio, which can be retrieved by Chen's [16] method. And α_c is extinction coefficient of the cirrus cloud.

$$\delta = \frac{\sigma_\pi^\perp}{\sigma_\pi^\parallel} = \frac{\beta_c^\perp}{\beta_c^\parallel} \quad (3)$$

Here, δ is the linear-depolarization ratio measured by the polarization lidars, which is determined from parallel and perpendicular polarization signals.

3. RESULTS

The case measured by LOSA-S lidar system to retrieve the properties of cirrus cloud is presented. The experimental backscatter signal was shown in red line of Figure 3, which was carried out on Mar. 30, 2013. Figure 3 also shows the backscatter color ratio and depolarization ratio of the measured cirrus cloud. From Figure 3 we can see that the cirrus cloud lies at the height of 6.8-9 km and the color ratios vary little with the height. The backscatter color ratio is an important parameter for cirrus clouds and reflects their shapes and size distribution information as is shown in Figure 3. From 6.8 to 9 km, in Figure 3 the averaged color ratios are about 0.7, and the depolarization ratio for this cirrus is 0.5 indicating the ice crystals are the main particles except for the height of 7.8 km with a deeply decreasing.

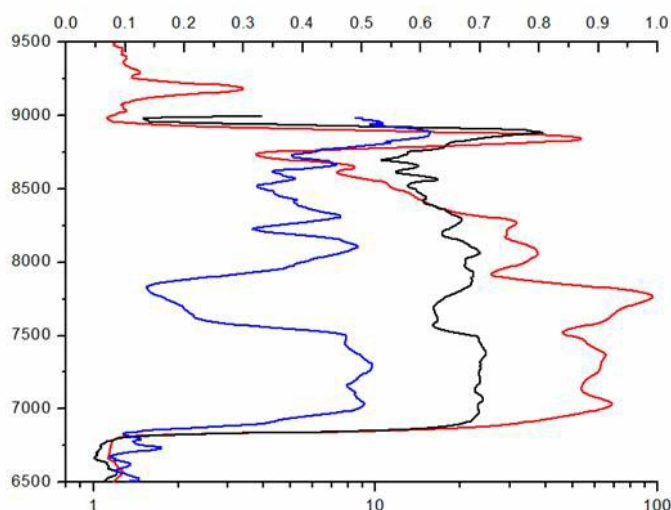


Figure 3. Simultaneous measurements of the depolarization ratio and color ratios by LOSA-S lidar (red: lidar signal at 532 nm; blue: depolarization ratio δ_{532} ; black: color ratio χ_{532}^{1064}) on Mar. 30, 2013.

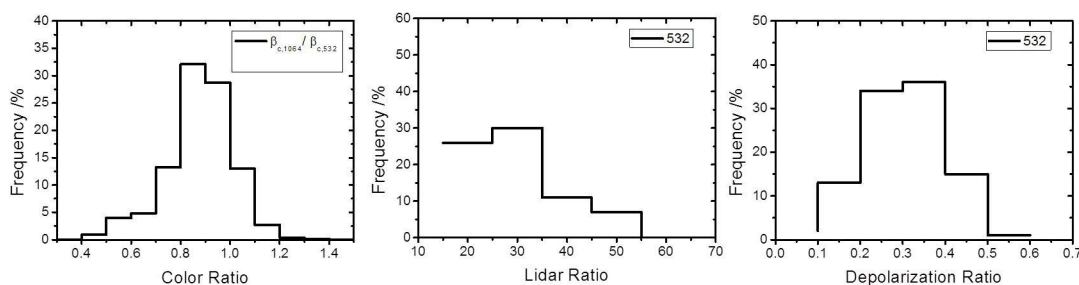


Figure 4. The frequency of lidar ratio, color ratio, and depolarization ratio for cirrus by TRMPL.

Table.1 Retrieved Parameters of the Measured Cirrus Cloud by TRMPL lidar

	Hefei
Color Ratio χ_{532}^{1064}	0.93
Lidar Ratio L_{532}	$29.7 \pm 9.8 \text{Sr}$
Depolarization Ratio δ_{532}	0.36 ± 0.12

The statistical characteristics of lidar ratio, color ratio, and depolarization ratio for cirrus cloud have been investigated using two years data over Hefei by the TRMPL lidar system, which are shown in Figure 4. And the retrieved parameters of the measured cirrus cloud are summarized in Table 1. The mean values for color ratio is 0.93 between 1064 and 532 nm wavelengths with the most frequency existing at 0.9. And the lidar ratios' mean value is 29.7 ± 9.8 Sr for 532. The averaged depolarization ratio is $0.360.36 \pm 0.12$ at 532 nm varying almost from 0.2 to 0.5.

From the case and statistical backscatter ratios, there are some difference of cirrus between Tomsk and Hefei. Many reasons will lead to this diversity, such as lidar tilt angle, regional aerosol condition, and as well as the sizes, shapes and orientation of the crystals in the clouds. As to light backscattering by cirrus, only some cases have been recently calculated by use of the physical-optics approximation [11]. The backscatter ratios for cirrus are quantified in theory and allow us to interrogate the microphysical properties of a cloud. Recently, Anatoli et al. [17] studied the impact of shape distortions of a hexagonal ice column on its backscattering properties at random particle orientation by use of the simplest geometrical model of the shape distortion. The backscatter ratios needed for interpretation of lidar signals are firstly calculated as functions of the distortion angles, which can explain the inconsistencies between the theoretical and experimental data. From Figure 5, when the distortion angle equals to about one, then the retrieved parameters of the measured cirrus cloud in Table 1 will be close to theory value.

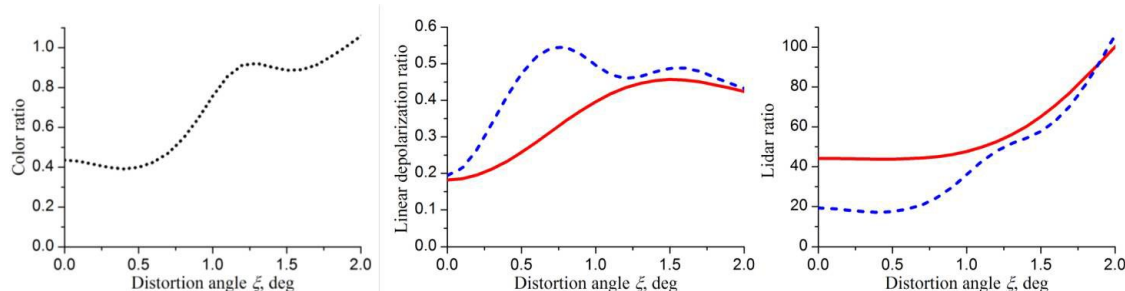


Figure 5. Backscatter ratios [17] for the randomly oriented column versus its distortion angle calculated in the physical-optics approximation for two wavelengths of 0.532 μm (dashed) and 1.064 μm (solid).

4. CONCLUSIONS

The properties of cirrus cloud by used observations obtained from the lidar system over Tomsk and Hefei. The backscatter ratios (polarization ratio, color ratio and lidar ratio) for cirrus cloud are compared with each other from these two regions. Some differences are found that are caused by detecting ways, aerosol conditions and cirrus itself. These differences can be mitigated by use of the appropriate microphysical model.

ACKNOWLEDGMENTS

This work is supported by the National Natural Science Foundation of China (under Grants No. 41305022, No. 41511130028 and No. 41590871), and is funded by Bureau of International Co-operation Chinese Academy of Sciences. A. Borovoi acknowledges the support by the Russian Foundation for Basic Research under Grants no. 15-05-06100 and no. 15-55-53081 and by the Chinese Academy of Sciences President's International Fellowship Initiative (No. 2016VEA044).

REFERENCES

- [1] Jensen, E. J., Toon, O. B., Selkirk, H. B., et al., "On the formation and persistence of subvisible cirrus clouds near the tropical tropopause," *J. Geophys. Res.* 101, 21361-21375 (1996).
- [2] Chen, T., Rossow, W. B., and Zhang, Y.-C., "Radiative effects of cloud-type variations," *J. Climate* 13, 264-286 (2000).
- [3] Nazaryan, H., McCormick, M. P., Menzel, W. P., "Global characterization of cirrus clouds using CALIPSO data," *J. Geophys. Res.* 113, D16211 (2008).
- [4] Goldfarb, L., Keckhut, P., Chanim, M. L., et al., "Cirrus climatological results from lidar measurements at OHP (44°N, 6°E)," *J. Geophys. Res. Lett.* 9(28), 1687-1690 (2001).
- [5] Noel, V., Chepfer, H., Ledanois, G., Delaval, A., and Flamant, P. H., "Classification of particle effective shape ratios in cirrus clouds based on the lidar depolarization ratio," *Appl. Opt.* 41(21), 4245-4257 (2002).

- [6] Chen, Wei-Nai, Chiang, Chih-Wei, and Nee, Jan-Bai, "Lidar ratio and depolarization ratio for cirrus clouds," *Appl. Opt.* 41(30), 6470-6476 (2002).
- [7] Wang, Z., Chi, R., Liu, B., and Zhou, J., "Depolarization properties of cirrus clouds from polarization LIDAR measurements over Hefei in spring," *Chinese Optics Letters* 6, 235-237 (2008).
- [8] Tao, Z., McCormick, M. P., Wu, D., Liu, Z., and Vaughan, M. A., "Measurements of cirrus cloud backscatter color ratio with a two-wavelength lidar," *Appl. Opt.* 47, 1478-1485 (2008).
- [9] Hayman, M., Spuler, S., and Morley, B., "Polarization lidar observations of backscatter phase matrices from oriented ice crystals and rain," *Opt. Express* 22(14), 16976-16990 (2014).
- [10] Borovoi, A., Balin, Y., Kokhanenko, G., Penner, I., Konoshonkin, A., Kustova, N., "Layers of quasi-horizontally oriented ice crystals in cirrus clouds observed by a two-wavelength polarization lidar," *Optics Express* 22(20), 24566-24573 (2014).
- [11] Borovoi, A., Konoshonkin, A., Kustova, N., "The physical-optics approximation and its application to light backscattering by hexagonal ice crystals," *J. Quant. Spectrosc. Radiat. Transfer* 146, 181-189 (2014).
- [12] Borovoi, A., Konoshonkin, A., and Kustova, N., "Backscattering by hexagonal ice crystals of cirrus clouds," *Opt. Lett.* 38, 2881-2884 (2013).
- [13] Borovoi, A., Konoshonkin, A., and Kustova, N., "Backscatter ratios for arbitrary oriented hexagonal ice crystals of cirrus clouds," *Opt. Lett.* 39(19), 5788-5791 (2014).
- [14] Balin, Yu., Kaul, B., Kokhanenko, G., and Winker, D., "Application of circularly polarized laser radiation for sensing of crystal clouds," *Opt. Express* 17(8), 6849-6859 (2009).
- [15] Liu, D., Tao, Z., Wu, D., and Wang, Z., "Development of Three-Wavelength Raman Polarization Lidar System and Case Study," *Acta Optica Sinica* 33(2), 0228001 (2013).
- [16] Chen, Wei-Nai, Chiang, Chih-Wei, and Nee, Jan-Bai, "Lidar ratio and depolarization ratio for cirrus clouds," *Appl. Opt.* 41(30), 6470-6476 (2002).
- [17] Borovoi, Anatoli, Kustova, Natalia, and Konoshonkin, Alexander, "Interference phenomena at backscattering by ice crystals of cirrus clouds," *Opt. Express* 23(19), 24557-24571 (2015).